Journal of Materials and Environmental Sciences
ISSN : 2028-2508

JMES, 2017 Volume 8, Issue 8, Page 2946-2955

http://www.jmaterenvironsci.com/

Use of *Lavandula Pedunculata* Essential Oil as a Green Corrosion Inhibitor for Mild Steel in 1 M Hydrochloric Acid Solution

S. Bouazama*[1], J. Costa[2], J. M. Desjobere[2], A. BenAli[3] A. Guenbour[1], A. Bellaouchou[1], A. Zarrouk[4] and M. Tabyaoui[1,*]

[1]*Laboratoire des Matériaux, Nanotechnologies et Environnement, Université Mohamed V , Faculté des Sciences, 4 Av. Ibn Battouta, B.P. 1014 RP, M-10000 Rabat, Morocco.*
[2]*Laboratoire de Chimie des Produits Naturels, Faculté des Sciences et techniques, Université de Corse, UMR CNRS6134, Corse, France*
[3]*Laboratoire Nationale de Contrôle des Médicaments (DMP). BP. 6206 Rabat Institut Maroc*
[4] *LC2AME, Faculty of Science, First Mohammed University, PO Box 717, 60 000 Oujda, Morocco.*

Received 16 Feb 2017,
Revised 05 Apr 2017,
Accepted 14 Apr 2017

Key words:

- ✓ Mild steel;
- ✓ HCl
- ✓ Corrosion inhibition;
- ✓ *Lavandula Pedunculata*;
- ✓ Weight loss
- ✓ Electrochemical techniques

S. Bouazama, M.Tabyaoui

soumiabouazama@gmail.com;
tabyaouihamid@gmail.com

Abstract

The *Lavandula Pedunculata* Essential Oil (LPEO) was tested as corrosion inhibitor of mild steel in 1M HCl medium using the weight loss measurements, potentiodynamic polarization and electrochemical impedance (EIS) methods. The analysis of essential oil from *Lavandula Pedunculata* essential oil was carried out by *gas chromatography*. The analysis of *Lavandula Pedunculata* essential oil showed that the major components were camphor (53.1%); 1.8-Cineole (6.5 %) and camphene (6.1 %). In temperature of 303K ,the inhibition efficiency increased with an increase in LPEO concentration, to attain 81% and 88 % at 3.0 g/L for methods of potentiodynamic polarization and electrochemical impedance (EIS) respectively. The obtained results revealed that the tested inhibitor leads to a systematic reduction in the kinetics of steel corrosion processes. It was found that LPEO behaved as a mixed type inhibitor. Electrochemical impedance spectroscopy (EIS) measurements show that charge transfer resistance (R_{ct}) increases and double-layer capacitance (C_{dl}) decreases in presence of inhibitor, suggesting the adsorption of the inhibitor molecules on the surface of mild steel. The studied process is found to be obeying to Langmuir model.

1. Introduction

The destruction of metallic materials due to the corrosion phenomenon is a serious industrial problem. Regarding the economic point of view, the replacement of corroded material constitutes a very high financial burden for industry [1-4]. The use of inhibitors is one of the most effective ways to prevent corrosion. Inhibitors are commonly used to reduce the corrosive attack of solutions to the contacted metallic materials [5]. The majority of well-known inhibitors are organic compounds containing heteroatoms such as O, N and S with multiple bonds. The efficiency of these organic corrosion inhibitors is related to the presence of polar functional groups with S, O and N atoms in the molecule [6-13]. Nevertheless, most of these organic compounds are not only expensive but also toxic to both human beings and the environment [14]. Therefore, the investigation of new cost-effective, non-toxic and eco-friendly inhibitors is essential to get over this problem and has been addressing toward the goal of using cheap, effective compounds at low or ‘‘zero’’ environmental impact. Natural products are nontoxic, biodegradable and readily available. They have been used widely as inhibitors. Many research groups have reported the successful use of naturally plant-derived substances to restrain the metal corrosion. [15-21].

The present work is devoted to test the *Lavandula Pedunculata* essential oil as corrosion inhibitor for mild steel in 1M HCl solution. The study is conducted by weight loss, potentiodynamic polarization and electrochemical impedance spectroscopy methods.

2. Experimental

2.1. *Plant material*

The *Lavandula Pedunculata* was collected during April 2013, from Tafraout in the South west of Morocco, Voucher specimens for plant were deposited in the Herbarium of the Laboratory of Plants in the Scientific Institute in Rabat, Morocco.

2.1.1. *Extraction of essential oil*

The studied essential oil was firstly extracted from the flowers and dry stalks of *Lavandula Pedunculata*. The apparatus used for the hydrodistillation is of type Clevenger, and then we added a desiccant (Na_2SO_4). The conservation of essential oils requires some essential precautions. For this reason we have stored them at a temperature close to 4°C, in a brown glass bottle tightly closed in order to protect it from light and air.

2.1.2. *Gas chromatography analysis (GC-FID)*

GC analysis was carried out using a Perkin-Elmer Autosystem XL GC apparatus (Waltham, MA, USA) equipped with a dual flame ionization detection (FID) system and the fused-silica capillary columns (60 m × 0.22 mm I.D., film thickness 0.25 μm) Rtx-1 (polydimethylsiloxane) and Rtx-wax (polyethyleneglycol). The oven temperature was programmed from 60 °C to 230 °C at 2 °C/min and then held isothermally at 230 °C for 35 min. Injector and detector temperatures were maintained at 280 °C. Samples were injected in the split mode (1/50) using helium as a carrier gas (1 mL/min) and a 0.2 μL injection volume of pure oil. Retention indices (RI) of compounds were determined relative to the retention times of a series of n-alkanes (C5-C30) (Restek, Lisses, France) with linear interpolation using the Van den Dool and Kratz equation [22] and software from Perkin-Elmer.

2.1.3. Gas chromatography mass spectrometry (GC-MS)

Samples were analyzed with a Perkin-Elmer turbo mass detector (quadrupole) coupled to a Perkin-Elmer Autosystem XL equipped with the fused-silica capillary columns Rtx-1 and Rtx-wax. Carrier gas: helium (1 mL/min), ion source temperature: 150 °C, oven temperature programmed from 60 °C to 230 °C at 2 °C/min and then held isothermally at 230 °C (35 min), injector temperature: 280 °C, energy ionization: 70 eV, electron ionization mass spectra were acquired over the mass range 35-350 Da, split: 1/80, injection volume: 0.2 μL of pure oil.

2.1.4. *Components identification*

Identification of individual components was based i) on comparison of calculated RI, on polar and apolar columns, with those of authentic compounds or literature data [23]; National Institute of Standards and Technology [24]; and ii) on computer matching with commercial mass spectral libraries [25]; and comparison of mass spectra with those of our own library of authentic compounds or literature data [23,25].

2.2. *Materials*

The steel used in this study is mild steel with a chemical composition: 0.179 wt. % C, 0.165 wt. % Si, 0.439 wt. % Mn, 0.203 wt. % Cu, 0.034 wt. % S and the remainder iron (Fe). The mild steel samples were pre-treated prior to the experiments by grinding with emery paper SiC (180, 320, 800, and 1200); rinsed with distilled water, degreased in acetone in an ultrasonic bath immersion for 5 min, washed again with bidistilled water and then dried at room temperature before use.

2.3. *Preparation of the solution*

The acids Acid solutions (1M HCl) were prepared by diluting a reagent of analytical grade HCl 37% with double-distilled water. The test solutions were freshly prepared before each experiment by adding *Lavandula Pedunculata* essential oil directly to the corrosive solution. Concentrations of *Lavandula Pedunculata* essential oil are 0.6, 1.2, 1.8, 2.4 and 3.0 g/L.

2.4. *Weight loss measurements*

Coupons were cut into 2 × 1 × 0.3 cm^3 dimensions are used for weight loss measurements. The surface of the test electrode was mechanically abraded by different grades of emery papers, washed with distilled water, cleaned with acetone after being weighed accurately with high sensitivity balance, the specimens were carried out in a double glass cell equipped with a thermostated cooling condenser containing 80 mL of non-de-aerated test solution with and without various concentrations of the studied compound at 303 K. After immersion period (6 h), the specimens were taken out, rinsed thoroughly with bidistilled water, dried and weighed accurately again. In order to get good reproducibility, parallel triplicate experiments were performed and the average weight loss value of three parallel mild steel sheets was obtained. The inhibition efficiency (E_W%) and surface coverage (θ) were calculated as follows:

$$\mathrm{E}_W(\%) = \left(1 - \frac{w_\mathrm{i}}{w_0}\right) \times 100 \qquad (1)$$

$$\theta = \left(1 - \frac{w_\mathrm{i}}{w_0}\right) \qquad (2)$$

where w_0 and w_i are the values of corrosion weight losses of mild steel in uninhibited and inhibited solutions, respectively, *A* the total area of the mild steel specimen (cm^2) and *t* is the exposure time (h).

2.5. *Electrochemical tests*

The electrochemical measurements were carried out using Volta lab (Tacussel- Radiometer PGZ 100) potentiostate and controlled by Tacussel corrosion analysis software model (Voltamaster 4) at under static condition. The corrosion cell used had three electrodes. The reference electrode was a saturated calomel electrode (SCE). A platinum electrode was used as auxiliary electrode of surface area of 1 cm^2. The working electrode was mild steel of the surface 1 cm^2. All potentials given in this study were referred to this reference electrode. The working electrode was immersed in test solution for 60 min to a establish steady state open circuit potential (E_ocp). After measuring the E_ocp, the electrochemical measurements were performed. The polarization curves are obtained from -600 mV to -300 mV and the scanning rate is of 2 mV / s.

All electrochemical tests have been performed in aerated solutions at 303 K. The EIS experiments were conducted in the frequency range with high limit of 100 kHz and different low limit 0.1 Hz at open circuit potential, with 10 points per decade, at the rest potential, after 60 min of acid immersion, by applying 10 mV ac voltage peak-to-peak. Nyquist plots were made from these experiments. The best semicircle can be fit through the data points in the Nyquist plot using a non-linear least square fit so as to give the intersections with the *x*-axis.

The inhibition efficiency of the inhibitor was calculated from the charge transfer resistance values using the following equation:

$$\mathrm{E}_{EIS}(\%) = \frac{R^i_{ct} - R^\circ_{ct}}{R^i_{ct}} \times 100 \qquad (3)$$

Where, R°_{ct} and R^i_{ct} are the charge transfer resistance in absence and in presence of inhibitor, respectively.

After ac impedance test, the potentiodynamic polarization measurements of mild steel substrate in inhibited and uninhibited solution were scanned from cathodic to the anodic direction, with a scan rate of 1 mV s^{-1}. The potentiodynamic data were analysed using the polarization VoltaMaster 4 software. The linear Tafel segments of anodic and cathodic curves were extrapolated to corrosion potential to obtain corrosion current densities (I_corr). From the polarization curves obtained, the corrosion current (I_corr) was calculated by curve fitting using the equation:

$$I = I_{corr}\left[exp\left(\frac{2.3\Delta E}{\beta_a}\right) - exp\left(\frac{2.3\Delta E}{\beta_c}\right)\right] \qquad (4)$$

The inhibition efficiency was evaluated from the measured I_corr values using the following relationship:

$$\mathrm{E}_\mathrm{I}(\%) = \frac{I_\mathrm{corr} - I_\mathrm{corr(i)}}{I_\mathrm{corr}} \times 100 \qquad (5)$$

where I_corr and $I_\mathrm{corr(i)}$ are the corrosion current densities for steel electrode in the uninhibited and inhibited solutions, respectively.

3. Result and discussion

3.1. *Composition of the essential oil*

The analysis of *Lavandula Pedunculata* Essential Oil (LPEO) has been carried out by CG. The chemical composition of essential oil was characterized by 32 compounds, which accounted for 87% of the total oil. The retention time of volatile compounds (*RI*a and *RI*p) and their percentage are summarized in Table 1.

Table 1: Composition of essential oil of *Lavandula Pedunculata*.

N	Compounds	Ir apol	Ir pol	HE% apol	Ir Bed
1	Tricyclene	922	1013	0.5	927
2	Alpha-pinene	932	1025	**2.0**	936
3	Camphene	946	1071	**6.1**	950
4	Thuja- 2.4 (10)diene	948	1127	0.3	946
5	B-pinene	973	1113	**1.4**	978
6	A-Terpinene	1011	1180	0.1	1013
7	P-cymenes	1014	1268	0.4	1015
8	1.8-Cineole	1024	1212	**6.5**	1024
9	Limonene	1024	1202	0.8	1025
10	G-Terpinene	1050	1245	0.1	1051
11	Camphenilone	1060	1453	0.4	
12	Fenchone	1071	1393	**1.3**	1069
13	Linalool oxide Z THF	1074	1436	0.4	1072
14	Camphor	1127	1511	**53.1**	1123
15	CIS-Verbenol	1132	1651	1.2	1132
16	P-mentha- 1.5 -dien-8-ol	1133	1669	0.3	1127
17	Pinocarvone	1142	1560	0.6	1137
18	Borneol	1152	1691	**1.5**	1150
19	Cryptone	1156	1656	0.5	1160
20	P-Cymen' Scheme-8-ol	1158	1833	0.7	1169
21	Myrtenal	1172	1618	0.8	1172
22	A-Terpineol	1174	1691	0.3	1176
23	Myrtenol	1182	1780	0.6	1178
24	Verbenone	1183	1714	**1.2**	1183
25	CIS-p-directed by P. Mentha-1 (7)8-dien-2-ol	1200	1898	0.5	1217
26	Cuminaldehyde	1214	1765	0.4	
27	Carvone	1217	1706	0.4	1214
28	Bornyl acetate	1270	1576	0.8	1270
29	Carvacrol	1280	2211	**1.2**	1278
30	B-Selinene	1481	1719	0.5	1486
31	1.10 -DI-epi-Cubenol	1603	2045	**1.2**	1615
32	B-Eudesmol	1635	2193	0.9	1641
			TOTAL	**87.0**	

RI *Bed* = retention indices on the apolar column of literature (König et al., 2001; National Institute of Standards and Technology, 2008)
RI *a* = retention indices on the apolar column (Rtx-1)
RI *p* = retention indices on the polar column (Rtx-Wax)

The oil was dominated by oxygenated monoterpenes (63 %), followed by monoterpenic hydrocarbons (28 %).The sesquiterpene hydrocarbons and oxygenated sesquiterpenes accounted only for 3% and 6% of the total oil, respectively. The essential oil has been characterized by a high amount of camphor (53.1 %). The other major components are: camphene (6, 1 %); 1.8-Cineole (6.5 %). The 30 other compounds are present in the (OLP) in low quantities.

It should be noted that several studies have been published on chemical composition of different kinds of *lavandula* .Verma et al. have studied the essential oil composition of *Lavandula officinalis* grown in Uttarakhand (India), they identified 37 monoterpene compounds. The major components were: linalyl acetate (47.56%), linalool (28.06%), lavandulyl acet ate (4.34%) and α- terpineol (3.7%) [26].

Lavandula officinalis in Kozajak (Macedonia) have also studied by Kulevanova et al., They found 32 components with noticeable dominance of Linalool (25.7%), linalyl acetate (23.2%) and lavandulyl acetate (12.4%) [27]

in another studies the essential oil composition of *Lavandula angustifolia* in Sydney, Australia dominated by linalool (43%), linalyl acetate (23%), camphor (8%) and borneol (6.6%).(L.T. Danh et al.) [28]

L. Hui et al. have also identified *lavandula angustufolia* in china and most predominant components are 1,5-Dimethyl-1-vinyl-4-hexenylbutyrate (43.73%), 1,3,7-Octatriene, 3,7-dimethyl- (25.10%), Eucalyptol (7.32%), and Camphor (3.79%) [29]. In general, this variation in the chemical composition can be understandable according to exogenous factors: the period of sunshine, the nature and the composition of the ground.

3.2. Corrosion tests

3.2.1. *Weight loss measurements*

Effect of concentration

The weight loss method has found broad practical application [30]. A major advantage of this method is its relative simplicity and availability. In addition, the method uses a direct parameter for the quantitative evaluation of corrosion, i.e., the loss in mass of the metal. The data obtained for the corrosion behavior of mild steel in 1M HCl solution with and without the addition of different concentrations of *Lavandula Pedunculata* Essential Oil (LPEO), after 6 h of immersion period at 303 K, are presented in table 2. The analysis of these results (Table 2) shows clearly that the weight loss decreases while the inhibition efficiency increases with increasing inhibitor concentration reaching a maximum value of 84% at a concentration of 3.0 g/L. This behavior can be attributed to the increase of the surface covered θ (E_W(%) /100), and that due to the adsorption of LPEO on the surface of the metal [31], as the inhibitor concentration increases.

Table 2: Efficiency and corrosion rate in the absence and presence of different concentrations of LPEO at 303 K.

C (g L^{-1})	W (mg cm^{-2} h^{-1})	E_W (%)	θ
Blank	0.846	—	—
0.6	0.482	43	0.43
1.2	0.367	57	0.57
1.8	0.305	64	0.64
2.4	0.230	73	0.73
3.0	0.135	84	0.84

Adsorption isotherm

The values of surface coverage to different concentrations of inhibitors, obtained from weight loss measurements at 303 K, have been used to explain the best isotherm to determine the adsorption process. Adsorption isotherms are very important in determining the mechanism of organo-electrochemical reactions [32]. The most frequently used isotherms are Langmiur, Temkin, Frumkin, Parsons, Hill de Boer, Flory-Huggins and Dahar-Flory-Huggins and Bockris-Swinkel [33-39]. All these isotherms are of the general form:

$$\int(\theta, x)\exp(2a\theta) = KC \qquad (6)$$

where $\int(\theta,x)$ is the configurational factor which depends upon the physical model and the assumptions underlying the derivation of the isotherm. "θ" is the surface coverage degree, "C" is the inhibitor concentration in the bulk of solution "a" is the lateral interaction term describing the molecular interactions in the adsorption layer and the heterogeneity of the surface. "K" is the adsorption-desorption equilibrium constant. The surface coverage θ for different concentrations of LPEO in 1M HCl at 303 K for 6 h of immersion time has been evaluated from weight loss. The data were tested graphically, see Fig. 1, by fitting to Langmuir isotherm which given by equation 7.

$$\frac{C}{\theta}=\frac{1}{K}+C \qquad (7)$$

where C is the equilibrium inhibitor concentration, K adsorptive equilibrium constant, θ representing the degree of adsorption (E_W%/100).

By far the best fit was obtained with the Langmuir isotherm (the strong correlation ($R^2 = 0.97$). The plots of C/θ vs. C yield a straight line (Fig. 1). This confirms that this inhibitor (LPEO) obeys Langmuir adsorption isotherm at 1M HCl medium. It indicates that the adsorbing LPEO species occupies typical adsorption site at the metal/solution interface. It is very important to note that discussion of the adsorption isotherm behavior using natural product extracts as inhibitors in terms of thermodynamic parameters (such as the standard free energy of adsorption value ΔG°_{ads}) is not possible because the molecular mass of the essential oil components is not known [39].

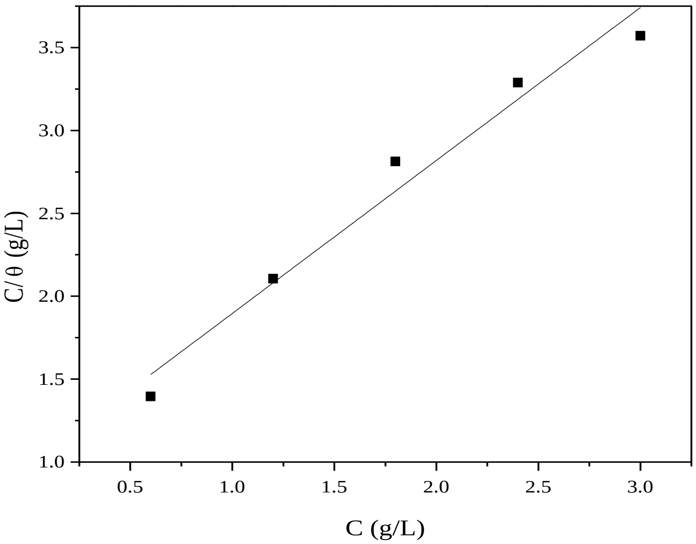

Figure 1: Langmuir isotherm adsorption of LPEO on the mild steel electrode in 1M HCl.

3.2.2. *Polarization study*

Figure 2 shows the Tafel curves in 1M HCl solutions with and without addition of LPEO at different concentrations. The corrosion current density decreases with increasing inhibitor concentrations and the corrosion potential shifts depending on the inhibitor concentration. The values of the electrochemical parameters obtained from the Tafel curves, namely: corrosion potential (E_{corr}), cathodic Tafel slope (β_c), anodic Tafel slope (β_a), corrosion current density (I_{corr}), inhibition efficiency E_I (%) for the different concentrations of LPEO are given in Table 3. It is clear that the addition of LPEO causes a decrease in the corrosion rate, i.e. shifts the cathodic and anodic curves to lower values of current densities. Namely, both cathodic and anodic reactions of mild steel electrode corrosion are inhibited by the inhibitor in acidic medium. This may be ascribed to adsorption of inhibitor over the corroded surface of mild steel [34]. It follows from the date of Table 3 that the corrosion current, I_{corr} decreases, while E_I (%) enhances with increase in inhibitor concentration. The decrease in the corrosion current density was observed for the LPEO, corresponding to a maximum efficiency of 81% at 3.0 g/L. Further inspection of Table 3 reveals that the presence of LPEO does not remarkably shift the E_{corr}, therefore, the selected compound can be described as mixed-type inhibitor for mild steel corrosion in 1M HCl, and the inhibition of the compound on mild steel is caused by adsorption, namely, the inhibition effect results from the reduction of the reaction area on the surface of the mild steel [35]. According to Ferreira et.al [36] and Li et. al. [37], if the displacement in corrosion potential is more than 85 mV with respect to the corrosion potential of the blank solution, the inhibitor can be consider as a cathodic or anodic type. In present study, maximum displacement was 57 mV with respect to the corrosion potential of the uninhibited sample which indicates that the studied inhibitor is a mixed type of inhibitor. The values of β_c slight changed, indicates that the cathodic corrosion mechanism of steel does not change. As it is shown in Fig. 2, cathodic current–potential curves give rise to parallel Tafel lines, which indicate that oxygen reduction reaction is activation controlled and that the addition of the LPEO.

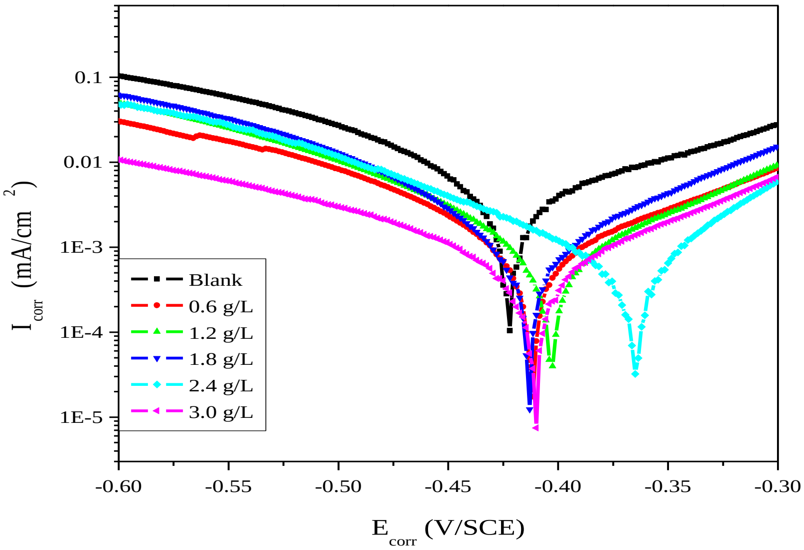

Figure 2: Polarization curves for mild steel in 1M HCl and various concentrations of LPEO at 303 K.

Table 3: Electrochemical parameters for mild steel in 1M HCl at different concentrations of LPEO at 303K.

Conc (g L^{-1})	$-E_{corr}$ (mV_{SCE})	I_{corr} (μA/cm²)	$-\beta_c$ (mV/dec)	β_a (mV/dec)	E_I (%)
Blank	422	491	83.0	110	—
0.6	411	254	80.0	99.8	48
1.2	402	212	84.0	83.0	57
1.8	413	169	50.4	61.6	66
2.4	365	128	78.9	48.6	74
3.0	409	93	71.2	69.8	81

3.2.3. *Electrochemical Impedance Spectroscopy (EIS)*

The Nyquist plots in the absence and presence of different studied concentrations of the LPEO are shown in Fig. 3. Nyquist plots give one semicircle in the absence and presence of different concentrations of LPEO suggesting that inhibition of metallic corrosion taking place in the present study is due to retardation of electron charge transfer process. Deviation from the perfect semicircle is generally attributed to the frequency dispersion as well as to the inhomogeneities of the surface and mass transport resistant [38]. Examination of the Fig. 3 shows that in the presence of LPEO the diameter of the Nyquist plots increases with increasing concentration. The increased diameter of the Nyquist plots in the presence of LPEO suggested that values of charged transfer resistance (R_{ct}) increase due to formation of protective film. The impedance parameters were derived using equivalent circuit described elsewhere [39] and are given in Table 4. The equivalent circuit consists of solution resistance (R_s), charge transfer resistance (R_{ct}) and a constant phase element (CPE) (Fig. 4), which consists of R_s solution resistance, R_{ct} charge transfer resistance and CPE constant phase elements for the double layer. A constant phase element (CPE) is used instead of a pure capacitor to compensate the non-ideal capacitive response of the interface and to get a more accurate fit of experimental data set. Its impedance is given by Eq. (8):

$$Z_{CPE} = \frac{1}{A(i\omega)^n} \tag{8}$$

Where A (Ω^{-1} s^n cm^{-2}) is the magnitude of the CPE, w (rad s^{-1}) is the sine wave modulation angular frequency, i^2 = -1 is the imaginary number and n is an empirical exponent which measures the deviation from the ideal capacitive behaviour [40,41]. Depending on the values of n, CPE can represent resistance (n = 0), capacitance (n = 1), inductance (n = -1) and Warburg impedance (n = 0.5) [42,43]. The values of R_{ct} in the absence and presence of different concentrations of LPEO were obtained by fitting EIS data in this equivalent circuit.

From the calculated values of R_{ct}, the value of double layer capacitance (C_{dl}) in the absence and presence of LPEO was calculated using the following equation [44]:

$$C_{dl} = \sqrt[n]{A\ (R_{ct})^{1-n}} \qquad (9)$$

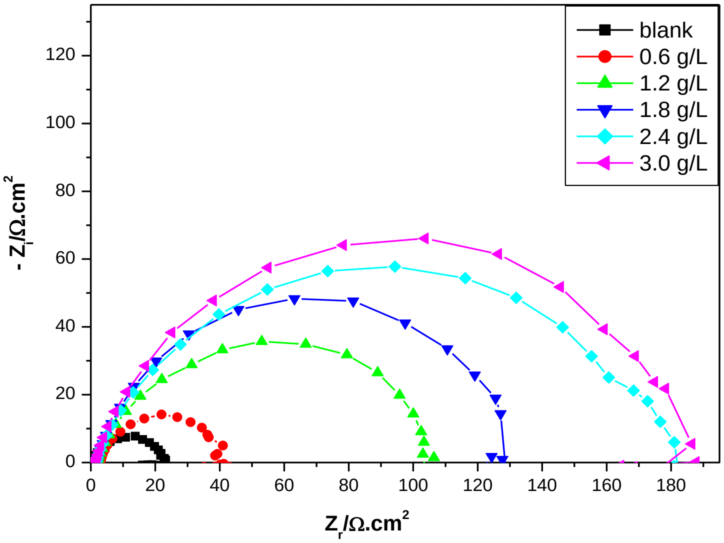

Figure 3: EIS Nyquist diagrams plots of mild steel in 1M HCl at different concentrations of LPEO at 303 K.

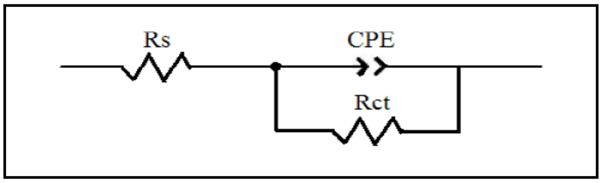

Figure 4: Electrical equivalent circuit used for modeling the interface mild steel/1M HCl solution without and with LPEO concentration.

Table 4: Impedance parameters for corrosion of mild steel in 1M HCl without and with different concentrations of LPEO at 303K.

Conc (g/L)	R_s (Ω cm^2)	R_{ct} (Ω cm^2)	C_{dl} (μF cm^{-2})	n	10^{-4}A (S^n/Ω cm^2)	E_{EIS} (%)
Blank	0.62	22.4	129.2	0.78	4.81	—
0.6	2.70	38.3	107.0	0.79	3.33	42
1.2	1.79	105	34. 4	0.79	1.12	78
1.8	1.89	128	39.6	0.80	1.14	82
2.4	1.47	174	21.8	0.76	0.83	87
3.0	1.49	186	19.7	0.75	0.80	88

Analyse of the impedance results in Table 4 shows that the charge-transfer resistance value, R_{ct}, increases with the concentration of LPEO and reaches a maximum value of 186 Ω cm^2 at 3.0 g/L. The increase in R_{ct} values demonstrates the improved protection effect of this compound and a slow corroding system, due to the gradual replacement of water molecules by LPEO molecules on the surface and consequently to a decrease in the number of active sites necessary for the corrosion reaction [45]. The value of the proportional factor A of CPE varies in a regular manner with inhibitor concentration. The decrease in C_{dl} can result from the decrease of the local dielectric constant or increase of thickness of electrical double layer, which suggest the substitution of H_2O molecules (with higher dielectric constant) with inhibitor molecules (with lower dielectric constant) leading to the formation of a thin protective film on the electrode surface [46]. However, the more the adsorption of inhibitor molecules on the metal surface, the more the thickness of the barrier layer is increased according to the expression of the Helmholtz model [47].

$$C_{dl} = \frac{\varepsilon_0 \varepsilon}{d} S \qquad (10)$$

where ε_0 is the permittivity of free space, ε is the local dielectric constant of medium, and S is the surface area of the electrode. Equation 10 suggests that C_{dl} is inversely proportional to the thickness of protective layer d.

Conclusion

The analysis of the essential oil of *Lavandula Pedunculata* shows that its composition is dominated by the camphor (53.1%), camphene (6.1%), 1.8-Cineole (6.5%). The *Lavandula pedunculata* essential oil (LPEO) of presents a good efficiency of the inhibition of the corrosion of the mild steel in hydrochloric acid 1M .This efficiency increases with the concentration of LPEO. The adsorption of LPEO on the mild steel surface follows the Langmuir adsorption isotherm. Data obtained from AC impedance technique show a frequency distribution and therefore a modelling element with frequency dispersion behaviour, a constant phase element (CPE) has been used. Based on the polarization results, the investigated *Lavandula pedunculata* essential oil (LPEO) can be classified as mixed inhibitor. The inhibition efficiencies determined by potentiodynamic polarization, electrochemical impedance spectroscopy and weight loss methods are in good agreement.

References

1. El Ouali, B., Hammouti, B., Aouiniti, A., Ramli, Y., Azougagh, M., Essasi, E.M., Bouachrine, M., *J. Mater. Environ. Sci*. 1 (2010)
2. Abd El Rehim, S.S., Ibrahim, M.A.M., Khaled, K.F., *J. Appl. Electrochem*. 29 (1999) 593.
3. Ghazoui A., Saddik R., Benchat N., Hammouti B., Guenbour M., Zarrouk A., . Ramdani M, Der Pharm. Chem. 2012, 4(1) 352.
4. Zarrok H., Saddik R., Oudda H., Hammouti B., El Midaoui A., Zarrouk A., Benchat N., Ebn Touhami M., *Der Pharm. Chem*. 2011, 3(5), 272.
5. Zarrouk A., Hammouti B., Touzani R., Al-Deyab S.S, Zertoubi M., Dafali A., Elkadiri S., *Int. J. Electrochem. Sci*., 6 (2011) 4939.
6. Zarrouk A., Hammouti B., Dafali A., Zarrok H., *Der Pharm. Chem*., 3(4) (2011) 266.
7. Ghazoui A., Zarrouk A., Bencaht N., Salghi R., Assouag M., El Hezzat M., Guenbour A., Hammouti B., *J. Chem. Pharm. Res*., 6(2) (2014) 704.
8. Zarrok H., Zarrouk A., Salghi R., Oudda H., Hammouti B., Assouag M., Taleb M., Ebn Touhami M., Bouachrine M., Boukhris S., *J. Chem. Pharm. Res*., 4(12) (2012) 5056.
9. Zarrok H., Zarrouk A., Salghi R., Assouag M., Hammouti B., Oudda H., Boukhris S., Al Deyab S.S., Warad I., *Der Pharm. Lett*., 5(2) (2013) 43.
10. Belayachi M., Serrar H., Zarrok H., El Assyry A., Zarrouk A., Oudda H., Boukhris S., Hammouti B., Ebenso E.E., Geunbour A., *Int. J. Electrochem. Sci*., 10(4) (2015) 3010.
11. Zarrouk A., Zarrok H., Salghi R., Touir R., Hammouti B., Benchat N., Afrine L.L., Hannache H., El Hezzat M., Bouachrine M., *J. Chem. Pharm. Res*., 5(12) (2013) 1482.
12. Zarrok H., Zarrouk A., Salghi R., Ebn Touhami M., Oudda H., Hammouti B., Touir R., Bentiss F., Al-Deyab S.S., *Int. J. Electrochem. Sci*., 8(4) (2013) 6014.
13. Ben Hmamou D., Aouad M.R., Salghi R., Zarrouk A., Assouag M., Benali O., Messali M., Zarrok H., Hammouti B., *J. Chem. Pharm. Res*. 2012, 4(7), 34984.
14. El-Etre A.Y., *Appl. Surf. Sci*. 252 (2006) 8521.
15. Hammouti B., Kertit S., Melhaoui A., *Bulletin of Electrochemistry* 13 (1997) 97-98
16. A. Bouoidina, F. El-Hajjaji, M. Chaouch, A. Abdellaoui, H. Elmsellem,Z. Rais, M. Filali Baba, A. Lahkimi, B. Hammouti and M. Taleb, *Der Pharma Chemica*, 8(13) (2016) 149-157

17. Abiola O.K., Otaigbe J.O.E., Kio O.J., *Corros. Sci*., 51 (2009) 1879.
18. Gunasekaran G., Chauhan L.R., *Electrochim. Acta*, 49 (2004) 4387.
19. Hamdani I., El Ouariachi E., Mokhtari O., Salhi A., Bouyanzer A., Zarrouk A., Hammouti B., J. Costa, *Der Pharm. Lett*., 7 (9) (2015) 109.
20. El bribri A, Tabyaoui M., Tabyaoui B., El Attari H., Bentiss F., *J . Mater. Chem. Phys.* (2013) 1-8
21. Hamdani I., El Ouariachi E., Mokhtari O., Salhi A., Chahboun N., ElMahi B., Bouyanzer A., Zarrouk A. , Hammouti B. , J. Costa, *Der Pharm. Chem.*, 7(8) (2015) 252.
22. Van den Dool H., Kratz P., *J. Chromatographie* 11 (1963) 463.
23. König W.A., Hochmuth D.H., Joulain D., Terpenoids and Related Constituents of Essential Oils. Library of Mass Finder 2.1 (Institute of Organic Chemistry, Hamburg, Germany, 2001).
24. National Institute of Standards and Technology. NIST WebBook (06/2005): http://webbook.nist.gov/chemistry.
25. Adams R.P., Identification of essential oil components by Gaz chromatography/quadrupole mass spectroscopy. *Allured Publishing*: (Carol Stream, 2001).
26. Verma Maiq R.S., Rahman U., Chanotiya Ch.S., Verma R.K., Amit Chauhan, Anju Yadav, Anand Sinhgh , Ajai K.Yadav *J. Serb. Chem. Soc.* (2010) *75* (3) 343–348
27. Kulevanova S., Stetkov G., M., Ristic. Examination .*Bulletin of the Chemists and Technologists of Macedonia*, 19 (2) (2000):165-169.
28. Danha L.T., Anh Triet N.D., Ngoc Han L.T., Zhao J., Mammucari R., Fostera N., *J. Supercrit. Fluids* 70 (2012) 27– 34
29. Hui L., He L., Huan L., XiaoLan L. , AiGuo Z., *African J. Microbiology Research* 4(4) (2010) 309-313, 18
30. Fomin M.N., Zhigalova K.A., Methods of Corrosion Testing of Metals. Metallurgiya, Moscow, 1986, pp.11-18
31. Singh A., Ahamad I., Singh V.K., Quraishi M.A., *J. Solid State Electrochem*. 2011, 15, 1087.
32. Wu X., Ma H., Chen S., Xu Z., Sui A., *J. Electrochem. Soc.* 1999, 146, 1847.
33. Langmuir I., *J. Am. Chem. Soc.* 1917, 39, 1848.
34. Alberty R., Silbey R., Physical Chemistry, second ed., Wiley, New York, 1997. p. 845.
35. Bockris J.O'M., Khan S.U.M., Surface Electrochemistry: A Molecular Level Approach, Plenum Press, New York, 1993.
36. Schapinik J.W., Oudeman M., Leu K.W., Helle J.N., *Trans. Farad. Soc.*, 56 (1960) 415.
37. Al Mamari K., Elmsellem H., Sebbar N. K., Elyoussfi A., Steli H., Ellouz M., Ouzidan Y., Nadeem A., Essassi E. M., El-Hajjaji F., *J. Mater. Environ. Sci.* 7 (9) (2016) 3286-3299.
38. Hill de Boer J., The Dynamical Character of Adsorption, second ed., Clarendon Press, Oxford, UK, 1986.
39. Dahmani M., Al-Deyab S.S., Et-Touhami A., Hammouti B., Bouyanzer A., Salghi R., A. ElMejdoubi1, Int. J. Electrochem. Sci., 7 (2012) 2513 - 2522.
34. Xia S., Qui M., Yu L., Lui F., *Corros. Sci*. 50 (2008) 2021.
35. Mu G.N., Li X.H., Qu Q., Zhou J., *Corros. Sci*. 48 (2006) 445.
36. Ferreira E.S., Giancomelli C., Giacomelli F.C., Spinelli A., *Mater. Chem. Phys.* 83 (2004) 129.
37. Li W.H., He Q., Pei C.L., Hou B.R., *J. Appl. Electrochem*. 38 (2008) 289.
38. Seikh A.H., Sherif E.M., *Int. J. Electrochem. Sci*. 10 (2015) 895.
39. Verma C.B., Reddy M.J., Quraishi M.A., *Anal. Bioanal. Electrochem.* 6 (2014) 321.
40. Lopez D.A., Simison S.N., de Sanchez S.R., *Electrochim. Acta.* 48 (7) (2003) 845.
41. Stoynov Z.B., Grafov B.M., Savova-Stoynova B., Elkin V.V., Electrochemical Impedance. Nauka. Moscow, 1991.
42. Musa A.Y., Kadhum A.A.H., Mohamad A.B., Takriff M.S., *Corros. Sci*. 52 (2010) 3331.
43. Zheng X., Zhang S., Li W., Yin L., He J., Wua J., *Corros. Sci.* 80 (2014) 383.
44. Shih H., Mansfeld F., *Corros. Sci.* 29 (1989) 1235.
45. Popova A., Raicheva S., Sokolova E., Christov M., *Langmuir* 12 (1996) 2083.
46. Ozcan M., Karadag F., Dehri I., *Colloids. Surf.* A 316 (2008) 55.
47. Ahamad I., Prasad R., Quraishi M.A., *J. Solid State Electrochem.* 14 (2010) 2095.

(2017); http://www.jmaterenvironsci.com/